ARMY RESEARCH LABORATORY

# Analysis of Bending a Square Ceramic Plate Under Strong Rotation

by Gene R. Cooper, Stephen A. Wilkerson, and Don Carlucci

ARL-TN-167 September 2000

The findings in this report are not to be construed as an official Department of the Army position unless so designated by other authorized documents.

Citation of manufacturer's or trade names does not constitute an official endorsement or approval of the use thereof.

Destroy this report when it is no longer needed. Do not return it to the originator.

**Army Research Laboratory**
Aberdeen Proving Ground, MD 21005-5066

**ARL-TN-167** **September 2000**

# Analysis of Bending a Square Ceramic Plate Under Strong Rotation

Gene R. Cooper and Stephen A. Wilkerson
Weapons and Materials Research Directorate, ARL

Don Carlucci
U.S. Army Armament Research, Development, and Engineering Center
Picatinny Arsenal, NJ

# Abstract

The U.S. Army has a continuing interest in smart weapons systems. Among them are projectiles employing independent logic. Smart weapons use printed circuitry with chips supplying the smarts for the system's autonomic functions. Experience has shown that considerable thought is required to design circuits that remain effective when subjected to severe environmental conditions. Launch conditions can place a projectile's components under axial loads as high as 40,000 g's, with spin rates up to 270 r/s and balloting loads up to 2,000 g's. Although short in duration, these loads can break even the most robust design. Unfortunately, when failure occurs, it is not obvious that a loading mechanism caused the problem, hence, making it difficult to make design corrections.

This report gives a simplified technique to determine if spin loading can break an internally housed chip. In particular, radial loading on the sense-and-destroy armor missile (SADARM) projectile's 68000 chip is examined. The methods employed here offer a quick means to eliminate potential problems, without employing sophisticated finite element techniques. Thin-plate theory is assumed adequate for determining stress levels in this chip, which is located off the rotation axis. Approximations for the chip's loading and boundary conditions are considered. Computational results are presented and examined.

# Table of Contents

INTENTIONALLY LEFT BLANK.

# List of Figures

INTENTIONALLY LEFT BLANK.

# List of Tables

INTENTIONALLY LEFT BLANK.

# 1. Introduction

A problem has surfaced with the 68000 ceramic (silicone) chip, found in the 155-mm sense-and-destroy armor missile (SADARM), breaking during or just after gun launch. The chip is a 2.4-cm square plate that is approximately 2 mm thick. Therefore, the plate length is relatively long in comparison to its thickness, having an aspect ratio of 12:1. Recent failures have been observed, where a fracture extends along the perpendicular bisector of one edge to the midpoint of the opposite edge. The chip is positioned in the projectile such that its geometric center is displaced approximately one-half radius from the projectile's symmetry axis. It is orientated so that its inner lateral face is parallel to this axis, with its bottom edge parallel to the projectile's base. Figure 1 depicts the loading as caused by projectile spin.

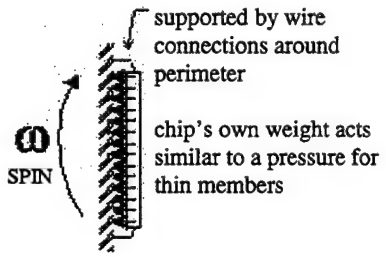


**Figure 1. Spin Loading of Chip.**

This failure pattern and orientation cause one to suspect that inertial spin forces are causing the chip to break. For these reasons, a study was made of the deformation of this chip due to a uniform load on its inner lateral surface, which is equal in magnitude to the inertial loading. Treating the chip as a thin rectangular plate allows one to model the bending characteristics with closed-form solutions of the familiar biharmonic boundary value problem. Two kinds of solutions were considered. First, it is assumed that the plate (chip) is simply supported. This is called the hinged plate. Next, the built-in plate (chip), referred to as the clamped plate, is examined. Since the actual chip is held in place with the usual integrated circuit solder and wire connections, these two cases should at least bracket the behavior of the contained chip. Physical differences between the cases are brought into the model by enforcing different sets of boundary

conditions. These two solutions can then be used to make reasonable predictions about the deformation of the 68000 chip found in SADARM caused by inertial spin loading.

A third cause would include an external pressure on the face of the chip from another structural component inside the projectile.* In this case, a uniform pressure has been included over half of the plate and the resulting stress levels have been calculated. The results from the previous analysis can be linearly combined with the new loading scenario, given that the chip is relatively brittle and that failure occurs near or at the yield point. This loading technique is graphically depicted in Figure 2.

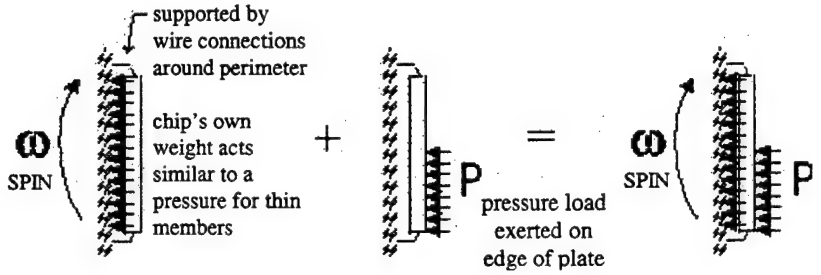


**Figure 2. Combination Loading of Chip.**

# 2. Mathematical Model

The model used in this report describes the bending of a thin rectangular plate subject to uniform loading. In particular, this plate is assumed to be undergoing constant circular motion with a spin rate equal to the maximum spin rate that the SADARM projectile experiences after gun launch. If the chip's thickness is thin relative to its length, then it is reasonable to assume that a nearly uniform load, q, is induced on the plate due to the mass of the chip and its rotation rate. The mass of the chip per unit area equals $\rho t$, where $\rho$ is the density of the chip and t is its thickness. The pressure load q is equal to the mass density times the acceleration, $r\omega^2$, where r is

* It was postulated that another component was deforming and applying pressure on half of the plate's surface. This additional pressure could have caused the observed failures.

the radius from the projectile's center of spin and $\omega$ is the angular rate.* Hence the resulting load is

$$q = \rho t \omega^2 r. \tag{1}$$

Following Timoshenko and Woinowsky-Krieger (1959) by placing the (x,y) coordinate plane on the midplane of the plate allows the governing equation for small deflections, w, to be written in the normal z direction as

$$\nabla^4 w = \frac{\partial^4 w}{\partial x^4} + 2\frac{\partial^4 w}{\partial x^2 \partial y^2} + \frac{\partial^4 w}{\partial y^4} = q/d, \tag{2}$$

where

$$d = \frac{E t^3}{12(1-\nu^2)} \tag{3}$$

and $\nabla^4$ is called the biharmonic operator. Equation (3) contains the chip modulus of elasticity E, thickness t, and Poisson's ratio $\nu$.

The two loading conditions (i.e., hinged plate and clamped plate) are modeled by two sets of boundary conditions applied to the solution of equation (2):

(1) the hinged plate, which has boundary conditions

$$w = 0$$

and

$$\frac{\partial^2 w}{\partial n^2} = 0 \tag{4}$$

*The angular rate of 1,696 radians/s was used in all of the calculations in this report. It is understood that higher rates are possible, depending on the muzzle velocity of the projectile.

on all sides (i.e., $|x| = \alpha$, $|y| = \alpha$); and

(2) the clamped plate, which has conditions

$$w = 0$$

and

$$\frac{\partial w}{\partial n} = 0 \tag{5}$$

on $|x| = \alpha$, $|y| = \alpha$, where n is the coordinate normal to the boundary. (See Figure 3.)

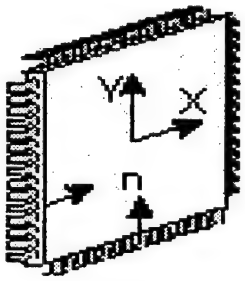


**Figure 3. Chip Coordinate System.**

Since the primary interest is material failure, the following stresses are calculated for each case:

$$\sigma_{xx} = -\frac{E t}{2\,(1-\nu^2)} \left( \frac{\partial^2 w}{\partial x^2} + \nu \frac{\partial^2 w}{\partial y^2} \right),$$

and

$$\sigma_{xy} = \frac{Et}{2(1+\nu)} \frac{\partial^2 w}{\partial x \partial y}. \tag{6}$$

The physical properties and loads used on the plate studied in this report are given in Table 1.

**Table 1. Physical Properties of the Ceramic Plate**

| Description | Value Used in Analysis |
|---|---|
| Load, q | 75 psi |
| Spin Rate, $\omega$ | 1,696 r/s |
| Plate Dimensions, a | 2.4 cm |
| Mean Radius, r | 138.75 mm |
| Elastic Modulus, E | 15,000,000 psi |
| Poisson's Ratio, $\nu$ | 0.23 |
| Plate Thickness, t | 2 mm |

The boundary value problem (BVP) for the hinged plate is easily solved using a double trigonometric series (Timoshenko and Woinowsky-Krieger 1959). Plotted results of these calculations including the stresses $\sigma_{xx}$ and $\sigma_{xy}$ are given in Figures 4–6.

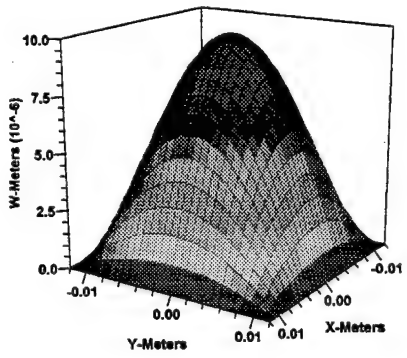


**Figure 4. Displacement Function for the Hinged Plate.**

The BVP for the clamped plate presents more mathematical difficulties than found for the hinged plate. The root of these difficulties stems from the requirement that both the displacement and its first derivative must be zero on the boundaries. Timoshenko and Woinowsky-Krieger (1959) give a series solution for this BVP that involves solving a system of linear equations for the undetermined coefficients. As a check on this procedure, two other methods of solving the same BVP were used. The first check was a Galerkin method, with selected functions that satisfy the boundary conditions (Ugural 1981). These calculations

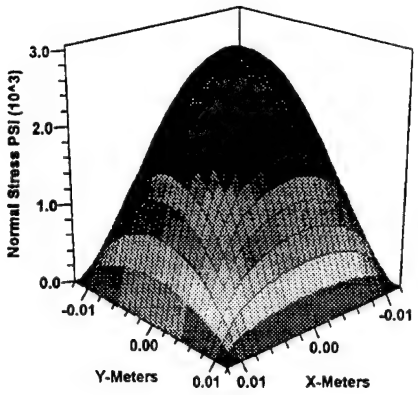


**Figure 5. Normal Stress $\sigma_{xx}$ Function for the Hinged Plate.**

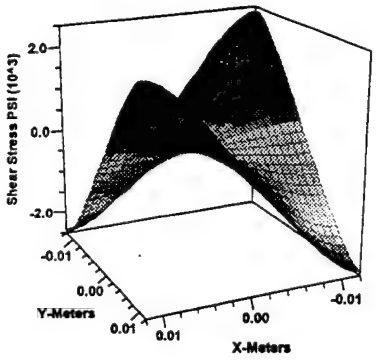


**Figure 6. Shear Stress $\sigma_{xy}$ Function for the Hinged Plate.**

produced a maximum displacement that was in good agreement with Timoshenko and Woinowsky-Krieger (1959), but, when the stresses were compared, their agreement was significantly less. This is not too surprising since higher derivatives associated with variational methods are generally suspect.

The second method for checking the solution constructs a series solution to the BVP using a sequence of complex biharmonic functions. This method requires the eigenvalues, z, of

$$\sin(z) + z = 0, \tag{7}$$

which can be found numerically (Morley 1963). Calculations using this method agreed well with Timoshenko and Woinowsky-Krieger (1959), but Timoshenko's method was found to be easier to use. Therefore, all plots presented here are the Timoshenko clamped-plate calculations. Figures 7–9 show the plotted displacement calculations plus the stresses $\sigma_{xx}$ and $\sigma_{xy}$ for the clamped plate.

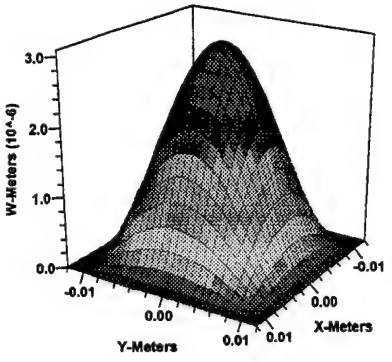


**Figure 7. Displacement Function for the Clamped Plate.**

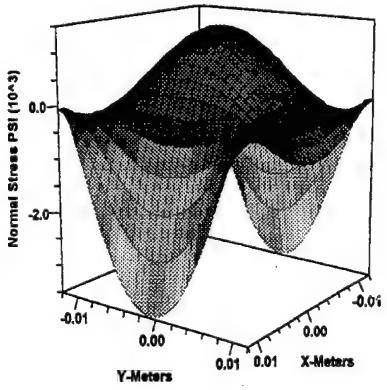


**Figure 8. Normal Stress $\sigma_{xx}$ Function for the Clamped Plate.**

The BVP for the clamped plate with an additional constant pressure distributed over half of the plate's surface is considered next. The same BVP and boundary conditions (6) used in case 2 describe this case. However, an additional uniform external pressure is now included on the right-hand side of equation (2), covering the region $0 < x < a$ and $0 < y < a/2$. It is further

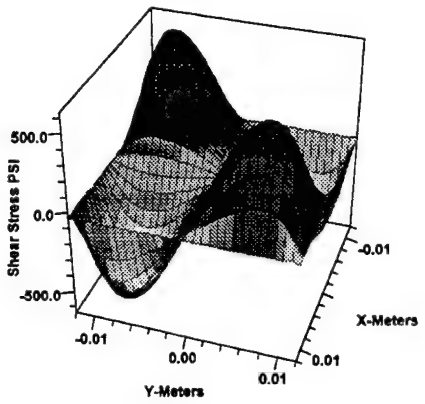


**Figure 9. Shear Stress $\sigma_{xy}$ Function for the Clamped Plate.**

assumed that this additional pressure distribution is equal to the inertial spin distribution used in the previous two cases (see Figure 2 or Figure 10).

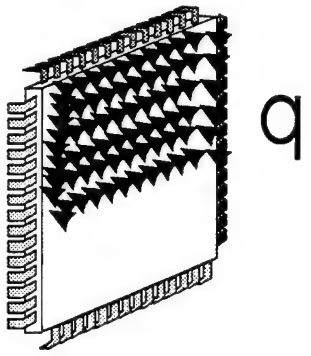


**Figure 10. Clamped Plate With Pressure on Half of the Surface.**

This means that the right-hand side of equation (2) becomes

$$q(1+\theta(y-a/2))/d, \tag{8}$$

where $\theta$ is the usual heavy-side step function. After expressing equation (8) as an appropriate trigonometric series, one can then use the previously discussed methods to solve this BVP. The calculations for this problem have the same functional shapes as those given for case 2, except that the magnitudes have changed, which reflects the additional half-plate pressure distribution.

In Figure 11, only the most important stress distribution, $\sigma_{xx}$, is displayed for the problem addressed here. For completeness, as well as ease of calculation, Table 2 presents expressions for calculating the maximum deflection and maximum $\sigma_{xx}$ for both the hinged and clamped square plate.

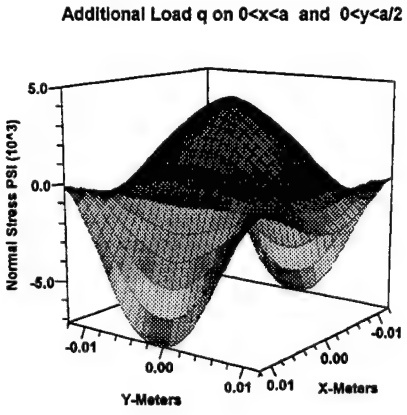


**Figure 11. Normal Stress $\sigma_{xx}$ Function for the Clamped Plate With Added Load.**

# 3. Conclusions

Inspection of the plots for both the hinged and clamped plate reveals that the most likely candidate causing the material failure previously described is the $\sigma_{xx}$ stress. In both cases, these calculations have the symmetry that best describes the centerline fractures most commonly found when the 68000 ceramic chip breaks. For clarification, the centerline $\sigma_{xx}$ that passes through the maximum stress points for both the hinged and clamped plates is plotted in Figures 12–14.

It is seen from these plots that the $\sigma_{xx}$ centerline values range from 1,600 psi to 5,000 psi. It has further been suggested that other internal components of SADARM may be pressing on the inner surface of the 68000 chip, making the load q larger than what has been used here. In the event that this takes place, one will find that the $\sigma_{xx}$ stress has the same general shape but that the magnitudes have increased.

**Table 2. Formula for the Plate Deflection and Stresses**

| Item | Plate Location | Formula |
|---|---|---|
| Maximum deflection for the hinged plate | Center | $w(0,0)=\frac{326\,\alpha^4 q}{80249d}$ |
| Maximum deflection for the clamped plate | Center | $w(0,0)=\frac{2013\alpha^4 q}{1590899d}$ |
| Maximum stress for the clamped plate | Center | $\sigma_{xx}\frac{Et(26930950v+v26947553)q\ \alpha^2}{30569831000d(1-v^2)}$ |
| Maximum stress for the clamped plate | Edge | $\sigma_{xx}(0,a/2)=\frac{1189q\alpha^2}{46354d(1-v^2)}Et$ |
| Maximum stress for the hinged plate | Center | $\sigma_{xx}\frac{Et(3468514v+v34696743)q\ \alpha^2}{1883310818d(1-v^2)}$ |
| Maximum deflection for the clamped plate with added load | Center | $w(0,0)=\frac{243\alpha^4 q}{72595d}$ |
| Maximum stress for the clamped plate with added load | Center | $\sigma_{xx}(0,0)=\frac{Et(17077867v+v18294720)q\,\alpha^2}{342368032(1-v^2)d}$ |
| Maximum plate with added load | Edge | $\sigma_{xx}(\frac{a}{2},0)=\frac{457q\ \alpha^2\ Et}{4316(1-v^2)d}$ |

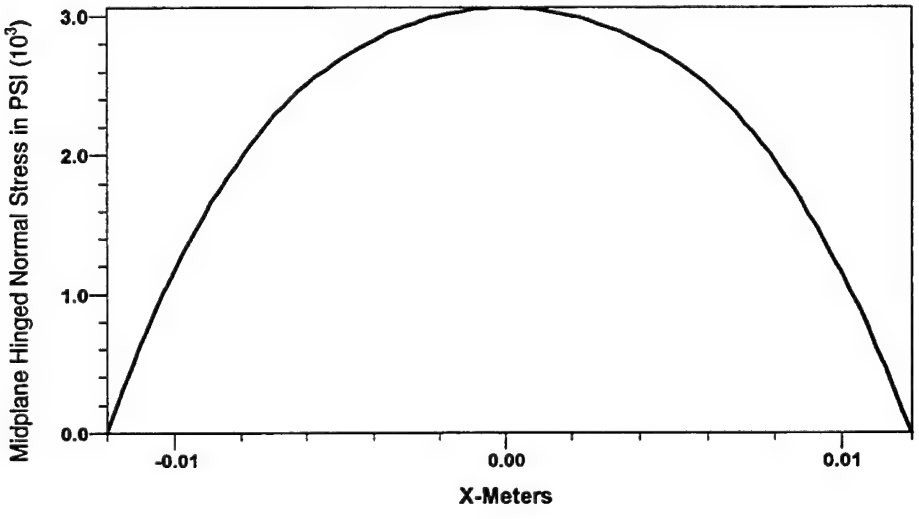


**Figure 12. Normal Stress $\sigma_{xx}$ Centerline Function for the Hinged Plate.**

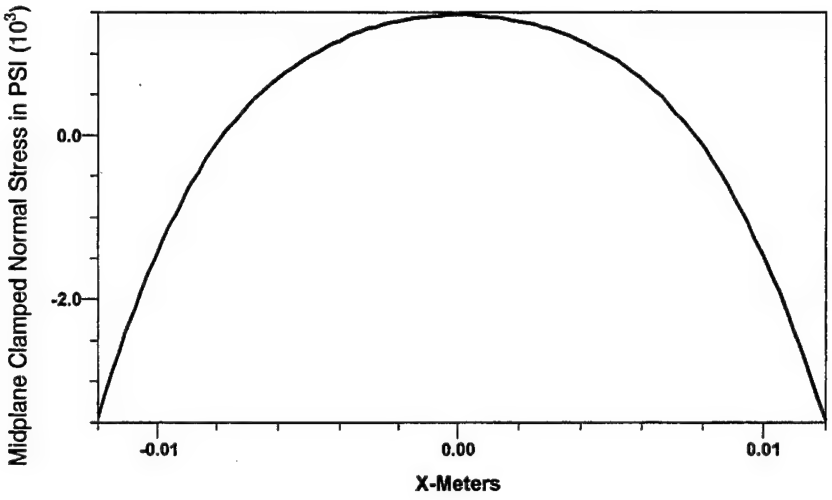


**Figure 13. Normal Stress $\sigma_{xx}$ Centerline Function for the Clamped Plate.**

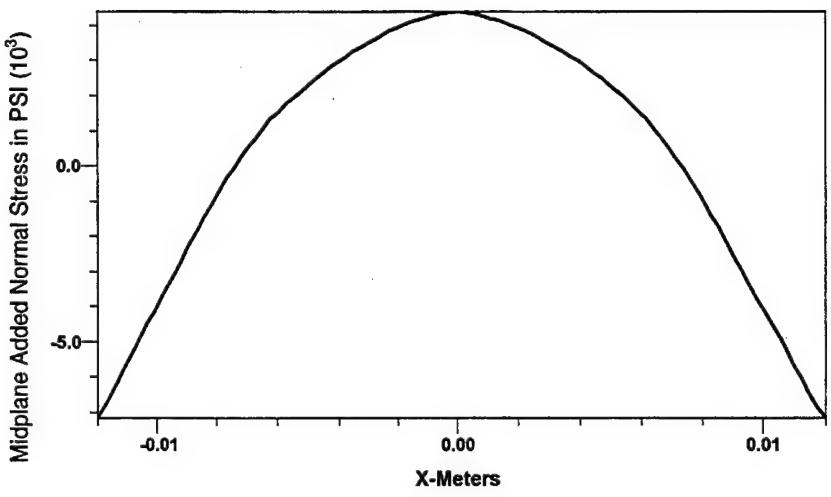


**Figure 14. $\sigma_{xx}$ Centerline Function for the Clamped Plate With Added Load.**

INTENTIONALLY LEFT BLANK.

# 4. References

Morley, L. S. "Simple Series Solution for the Bending of a Clamped Rectangular Plate Under Uniform Normal Load." *The Quarterly Journal of Mechanics and Applied Mathematics*, vol. XVI, February 1963.

Timoshenko, S., and Woinowsky-Krieger, S. *Theory of Plates and Shells*. McGraw-Hill, 1959.

Ugural, A. C. *Stresses in Plates and Shells*. McGraw-Hill, 1981.

INTENTIONALLY LEFT BLANK.

# List of Symbols

| | |
|---|---|
| a | Edge lengths of rectangular plate |
| d | Flexural rigidity of the plate |
| E | Elastic modulus |
| q | Uniform normal load |
| r | Mean radius from projectile symmetry axis |
| t | Plate thickness |
| w | Normal deflection of the plate |
| x, y, z | Cartesian coordinates |
| $\upsilon$ | Poisson's ratio |
| $\rho$ | Mass density |
| $\sigma_{xx}$ | Stress in x direction in a plane normal to the x axis |
| $\sigma_{xy}$ | Stress in x direction in a plane normal to the y axis |
| $\omega$ | Projectile spin rate |

INTENTIONALLY LEFT BLANK.

| NO. OF COPIES | ORGANIZATION |
|---|---|
| 2 | DEFENSE TECHNICAL<br>INFORMATION CENTER<br>DTIC DDA<br>8725 JOHN J KINGMAN RD<br>STE 0944<br>FT BELVOIR VA 22060-6218 |
| 1 | HQDA<br>DAMO FDT<br>400 ARMY PENTAGON<br>WASHINGTON DC 20310-0460 |
| 1 | OSD<br>OUSD(A&T)/ODDDR&E(R)<br>R J TREW<br>THE PENTAGON<br>WASHINGTON DC 20301-7100 |
| 1 | DPTY CG FOR RDA<br>US ARMY MATERIEL CMD<br>AMCRDA<br>5001 EISENHOWER AVE<br>ALEXANDRIA VA 22333-0001 |
| 1 | INST FOR ADVNCD TCHNLGY<br>THE UNIV OF TEXAS AT AUSTIN<br>PO BOX 202797<br>AUSTIN TX 78720-2797 |
| 1 | DARPA<br>B KASPAR<br>3701 N FAIRFAX DR<br>ARLINGTON VA 22203-1714 |
| 1 | NAVAL SURFACE WARFARE CTR<br>CODE B07 J PENNELLA<br>17320 DAHLGREN RD<br>BLDG 1470 RM 1101<br>DAHLGREN VA 22448-5100 |
| 1 | US MILITARY ACADEMY<br>MATH SCI CTR OF EXCELLENCE<br>MADN MATH<br>MAJ HUBER<br>THAYER HALL<br>WEST POINT NY 10996-1786 |

| NO. OF COPIES | ORGANIZATION |
|---|---|
| 1 | DIRECTOR<br>US ARMY RESEARCH LAB<br>AMSRL D<br>D R SMITH<br>2800 POWDER MILL RD<br>ADELPHI MD 20783-1197 |
| 1 | DIRECTOR<br>US ARMY RESEARCH LAB<br>AMSRL DD<br>2800 POWDER MILL RD<br>ADELPHI MD 20783-1197 |
| 1 | DIRECTOR<br>US ARMY RESEARCH LAB<br>AMSRL CI AI R (RECORDS MGMT)<br>2800 POWDER MILL RD<br>ADELPHI MD 20783-1145 |
| 3 | DIRECTOR<br>US ARMY RESEARCH LAB<br>AMSRL CI LL<br>2800 POWDER MILL RD<br>ADELPHI MD 20783-1145 |
| 1 | DIRECTOR<br>US ARMY RESEARCH LAB<br>AMSRL CI AP<br>2800 POWDER MILL RD<br>ADELPHI MD 20783-1197 |
| | ABERDEEN PROVING GROUND |
| 4 | DIR USARL<br>AMSRL CI LP (BLDG 305) |

INTENTIONALLY LEFT BLANK.

# REPORT DOCUMENTATION PAGE

*Form Approved*
*OMB No. 0704-0188*



| 1. AGENCY USE ONLY *(Leave blank)* | 2. REPORT DATE | 3. REPORT TYPE AND DATES COVERED |
|---|---|---|
| | September 2000 | Final, Feb–Jul 98 |

**4. TITLE AND SUBTITLE**

Analysis of Bending a Square Ceramic Plate Under Strong Rotation

**5. FUNDING NUMBERS**

1L1622618AH80

**6. AUTHOR(S)**

Gene R. Cooper, Stephen A. Wilkerson, and Don Carlucci*

**7. PERFORMING ORGANIZATION NAME(S) AND ADDRESS(ES)**

U.S. Army Research Laboratory
ATTN: AMSRL-WM-BC
Aberdeen Proving Ground, MD 21005-5066

**8. PERFORMING ORGANIZATION REPORT NUMBER**

ARL-TN-167

**9. SPONSORING/MONITORING AGENCY NAMES(S) AND ADDRESS(ES)**

**10.SPONSORING/MONITORING AGENCY REPORT NUMBER**

**11. SUPPLEMENTARY NOTES**

* U.S. Army Armament Research, Development, and Engineering Center, Picatinny Arsenal, NJ 07806-5000

**12a. DISTRIBUTION/AVAILABILITY STATEMENT**

Approved for public release; distribution is unlimited.

**12b. DISTRIBUTION CODE**

**13. ABSTRACT** *(Maximum 200 words)*

The U.S. Army has a continuing interest in smart weapons systems. Among them are projectiles employing independent logic. Smart weapons use printed circuitry with chips supplying the smarts for the system's autonomic functions. Experience has shown that considerable thought is required to design circuits that remain effective when subjected to severe environmental conditions. Launch conditions can place a projectile's components under axial loads as high as 40,000 g's, with spin rates up to 270 r/s and balloting loads up to 2,000 g's. Although short in duration, these loads can break even the most robust design. Unfortunately, when failure occurs, it is not obvious that a loading mechanism caused the problem, hence, making it difficult to make design corrections.

This report gives a simplified technique to determine if spin loading can break an internally housed chip. In particular, radial loading on the sense-and-destroy armor missile (SADARM) projectile's 68000 chip is examined. The methods employed here offer a quick means to eliminate potential problems, without employing sophisticated finite element techniques. Thin-plate theory is assumed adequate for determining stress levels in this chip, which is located off the rotation axis. Approximations for the chip's loading and boundary conditions are considered. Computational results are presented and examined.

**14. SUBJECT TERMS**

ceramic plate, hypergeometric, variational method

**15. NUMBER OF PAGES**

19

**16. PRICE CODE**

| 17. SECURITY CLASSIFICATION OF REPORT | 18. SECURITY CLASSIFICATION OF THIS PAGE | 19. SECURITY CLASSIFICATION OF ABSTRACT | 20. LIMITATION OF ABSTRACT |
|---|---|---|---|
| UNCLASSIFIED | UNCLASSIFIED | UNCLASSIFIED | UL |

INTENTIONALLY LEFT BLANK.

## USER EVALUATION SHEET/CHANGE OF ADDRESS

This Laboratory undertakes a continuing effort to improve the quality of the reports it publishes. Your comments/answers to the items/questions below will aid us in our efforts.

1. ARL Report Number/Author ARL-TN-167 (Cooper) Date of Report September 2000

2. Date Report Received _____

3. Does this report satisfy a need? (Comment on purpose, related project, or other area of interest for which the report will be used.) _____

4. Specifically, how is the report being used? (Information source, design data, procedure, source of ideas, etc.) _____

5. Has the information in this report led to any quantitative savings as far as man-hours or dollars saved, operating costs avoided, or efficiencies achieved, etc? If so, please elaborate. _____

6. General Comments. What do you think should be changed to improve future reports? (Indicate changes to organization, technical content, format, etc.) _____

CURRENT ADDRESS

_____
Organization

_____
Name E-mail Name

_____
Street or P.O. Box No.

_____
City, State, Zip Code

7. If indicating a Change of Address or Address Correction, please provide the Current or Correct address above and the Old or Incorrect address below.

OLD ADDRESS

_____
Organization

_____
Name

_____
Street or P.O. Box No.

_____
City, State, Zip Code

(Remove this sheet, fold as indicated, tape closed, and mail.)
**(DO NOT STAPLE)**